The Spallation Neutron Source Project – Physical and Technical Challenges[1]

Jie Wei[2]

for the Spallation Neutron Source Collaboration, USA

Abstract. The Spallation Neutron Source (SNS) is designed to reach an average proton beam power of 1.4 MW for pulsed neutron production. This paper summarizes design aspects and physical challenges to the project.

CONTENTS

INTRODUCTION

The SNS project, designed to reach an average beam power above 1.4 MW for pulsed neutron production, is presently in the fourth year of a seven-year construction cycle at ORNL (Fig. 1) [1]. The accelerator system operates at a repetition rate of 60 Hz and an average current of 1.6 mA. It consists of an H^- RF volume source of 48 mA peak current at 6% duty, a low-energy beam transport (LEBT) housing a first-stage beam chopper with ±20 ns rise/fall time; a 402.5 MHz, 4-vane radio-frequency-quadrupole (RFQ); a medium-energy beam transport (MEBT) housing a second-stage chopper ($< \pm10$ ns rise/fall), an adjustable beam-halo scraper, diagnostics devices, and matching quadrupoles; a 402.5 MHz, 6-tank drift-tube-linac (DTL) with permanent-magnet quadrupoles; a 805 MHz, 4-module coupled-cavity-linac (CCL); a 805 MHz, superconducting RF (SRF) linac of
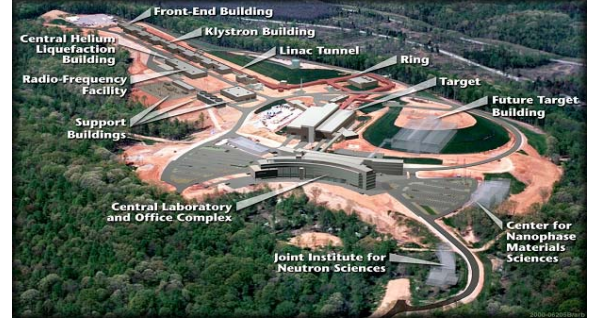

FIGURE 1. Layout of the Spallation Neutron Source.

TABLE 1. Spallation Neutron Source primary parameters.

	Baseline	Back-up
Kinetic energy, E_k [MeV]	1000	975
Uncertainty, ΔE_k (95%) [MeV]	±15	±15
SRF cryo-module number	$11+12$	$11+15$
SRF cavity number	$33+48$	$33+60$
Peak field E_p ($\beta=0.61$) [MV/m]	27.5	27.5
ΔE_p ($\beta=0.61$) [MV/m]	±2.5	±2.5
Peak field E_p ($\beta=0.81$) [MV/m]	35	27.5
ΔE_p ($\beta=0.81$) [MV/m]	$+2.5/-7.5$	±2.5
Beam power on target, P_{max} [MW]	1.4	1.7
Pulse length on target [ns]	695	699
Chopper beam-on duty factor [%]	68	68
Linac macro pulse duty factor [%]	6.0	6.0
Ave. macropulse H^- current [mA]	26	32
Linac ave. beam current [mA]	1.6	1.9
Ring rf frequency [MHz]	1.058	1.054
Ring injection time [ms]	1.0	1.0
Ring bunch intensity [10^{14}]	1.6	1.9
Ring space-charge tune spread	0.15	0.20

medium- and high-β cavities accelerating the beam to the full energy; a high-energy beam transport (HEBT) for diagnostics, transverse and longitudinal collimation, matching, energy correction and painting; and an accumulator ring compressing the 1 GeV, 1 ms pulse to 650 ns for delivery onto the target through a ring-target beam transport (RTBT).

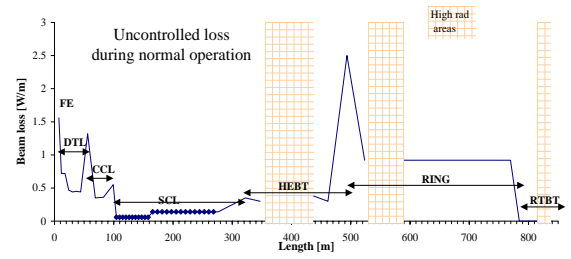Table 1 lists major parameters. The energy acceptance of the ring is about ±50 MeV, mainly due to conditions

---

TABLE 2. Beam parameter evolution across the SNS accelerators. The aperture and acceptance do not include scrapers and collimators. Notes are: a) corresponding to 27% chopped beam; b) corresponding to 5% chopped beam; c) beam loss on the transverse and momentum collimators; d) including total 4% of beam escaping foil and 0.2 and f) corresponding to 20% beam loss averaged over RFQ length.

	Baseline LEBT	Back-up RFQ	MEBT	DTL	CCL	SRF 1	SRF 2	HEBT	Ring	RTBT	Unit
E_k (out)	0.065	2.5	2.5	86.8	185.6	387	1000	1000	1000	1000	MeV
Length	0.12	3.8	3.6	36.6	55.1	64.2	94.7	169.5	248.0	150.8	m
Peak current	47	38	38	38	38	38	38	38	9×10^4	9×10^4	mA
Min. trans. aperture		7	32	25	30	80	80	50	200		mm
Min. H acceptance			250	38	19	57	50	26	480	480	μm
H emit. out, $\varepsilon_{un,rms}$	17	2.9	3.7	0.75	0.59	0.41	0.23	0.26	24	24	μm
Min. V acceptance			51	42	18	55	39	26	480	400	μm
V emit. out, $\varepsilon_{un,rms}$	17	2.9	3.7	0.75	0.59	0.41	0.23	0.26	24	24	μm
Min. L acceptance			4.7	2.4	7.4	7.2	18		$19 \times 10^5/\pi$		$10^{-5}\,\pi$eVs
L emit. out, rms		7.6	10	12	14	17	23		$2 \times 10^7/\pi$		$10^{-7}\,\pi$eVs
Loss (control)	0.05^a	N/A	0.2^b	N/A	N/A	N/A	N/A	5^c	62^d	58^e	kW
Loss (uncontroll)	70	100^f	2	1	1	0.2	0.2	<1	1	<1	W/m
H emit. out, $\varepsilon_{N,rms}$	0.2	0.21	0.27	0.33	0.39	0.41	0.41	0.46	44	44	μm
V emit. out, $\varepsilon_{N,rms}$	0.2	0.21	0.27	0.33	0.39	0.41	0.41	0.46	44	44	μm

Source: N. Catalan-Lasheras, et al

FIGURE 2. Expected beam loss across the SNS accelerator complex. The uncontrolled beam loss is at 1 W/m level.

DESIGN PHILOSOPHY

The primary concern is that radio-activation caused by excessive uncontrolled beam loss can limit the machine's availability and maintainability. Based on operational experiences, hands-on maintenance demands that the average uncontrolled beam loss does not exceed 1 W beam power per tunnel-meter [2]. Uncontrolled losses are usually attributed to 1) mismatch upon change of linac structure, lattice, and frequency; 2) space-charge effects including envelope and parametric resonances and non-equipartition in the linac, and resonance crossing and instability enhancement in ring; 3) limited physical and momentum acceptance; 4) premature H^- and H^0 stripping and ring injection foil scattering; 5) magnetic errors, fringe fields, and misalignments; 6) instabilities (resistive impedances due to e.g. extraction kicker, and electron cloud); and 7) accidental loss due to system malfunction (ion source and linac, ring extraction kickers).

SNS addresses the above seven issues by adopting a low-loss design philosophy [3]. Above all, foreseen losses are localized to shielded areas using 1) adjustable scrapers in the MEBT; 2) transverse and momentum collimators in the HEBT prior ring injection; 3) two-stage transverse collimation and momentum cleaning with beam-in-gap (BIG) kicker in the ring; 4) collimator protection in the RTBT, and 5) beam-gap cleaning with LEBT and MEBT choppers and ring BIG kicker (Fig. 2).

Emphasis is also put on machine's flexibility and reliability. The SRF linac allows operation with one failed cavity/klystron; the ring accepts ±5% variation in linac output energy; a wide ring tuning range avoids resonances; a robust injection allows independent horizontal, vertical, and longitudinal painting; adjustable collimation systems accommodate variable beam size; and design reserve and redundancy ensure a high availability (e.g., spare cryo-module for a quick replacement, power supplies compatible with 1.3 GeV energy, multi-foil exchange, spare kicker power supply (PFN), and aperture clearance for one-kicker failure).

Finally, the facility is designed with the potential to reach a beam energy up to 1.3 GeV and a beam power higher than 2 MW, capable of supplying a second neu-

for a tolerable H^- and H^0 stripping loss. The back-up scenario corresponds to the case if the surface field of the SRF cavity is lower than expected (37.5 MV/m). Extra tunnel space (71 m) is reserved to extend the linac length for a higher output energy. Table 2 shows evolution of beam parameters during the cycle including expected energy, horizontal (H), vertical (V), and longitudinal (L) acceptances and emittances, and controlled and uncontrolled beam losses.
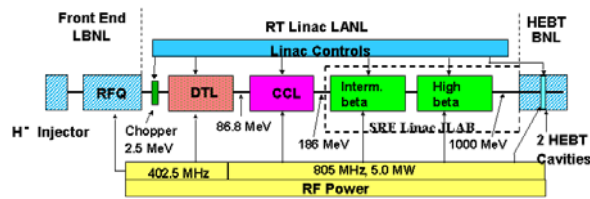
FIGURE 3. SNS front-end and linac stucture.

tron target. The higher energy can be reached by upgrading the superconducting RF cavity gradient and klystron power supplies, and by filling the presently unoccupied linac tunnel spaces with up to 9 additional cryo-modules. The ring is capable of accommodating the energy and power increase without extensive hardware change – space is reserved for two additional extraction kickers, and for the replacement of 2 injection-chicane dipoles to satisfy H^0 stripping conditions [4].

ACCELERATOR DESIGN CHOICES

Superconducting vs. Warm Linac

The SRF linac operating at 805 MHz frequency accelerates the H^- beam from 186 MeV to top energy (Fig. 3). Comparing with the original normal-conducting (warm) CCL linac, the SRF linac provides a high accelerating gradient (11 - 16 MV/m) capable of reaching a higher beam energy, encounters less beam loss and halo scraping due to its larger bore radius, is immune to one cavity/klystron failure, operates at a better vacuum, and is expected to have higher reliability and availability. The selection of two types of SRF cavities allows for economic savings and future energy upgrades. On the other hand, the relatively large phase slip requires detailed error-sensitivity analysis. The choice of cavity geometric β value is based on a smooth transition from the warm section linac, a maximized final output energy, and a comfortable transition from medium- to high-β section with tolerance to one cavity failure. We also choose constant-gradient, continuous focusing to maximize the accelerating field strength [5].

Considering the tight construction schedule, a moderate peak surface field of 27.5 MV/m is chosen for the medium-β cavity. Benefiting from electro-polishing, a higher peak field of 35 MV/m is assumed for the high-β cavity. In order to reduce uncertainties in RF controls of an ion ($\beta < 1$) beam under Lorentz detuning, microphonics, beam transients and injecting energy offset, we decide to drive each cavity with its own klystron using independent amplitude and phase control.

Accumulator Ring vs. RCS

During the first year of construction, a study was performed comparing the present structure of full-
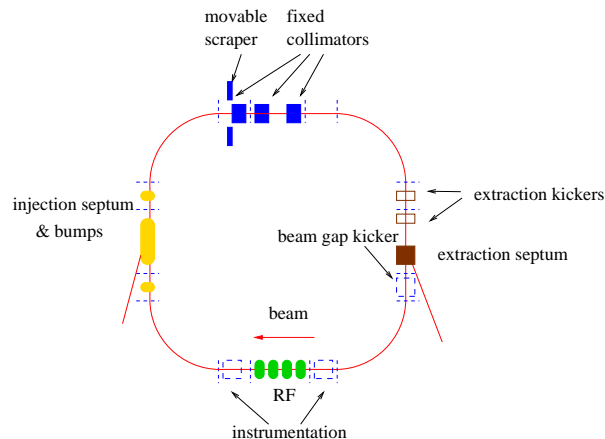

FIGURE 4. SNS accumulator ring layout.

energy linac plus accumulator ring to a rapid-cycling-synchrotron (RCS) design: a 60 Hz, 400 MeV linac feeds two, vertically stacked RCSs accelerating the proton beam to 2 GeV energy. The biggest challenge to the RCS design is from the stringent (1 W/m) beam-loss criterion: although relaxed by a factor of 5, still only 0.4% uncontrolled loss is allowed for a 2 MW beam power assuming 90% collimation efficiency. On the other hand, among existing rings the lowest loss of about 0.3% is achieved at LANL's PSR, a 800 MeV accumulator, as opposed to typical losses of a few to tens of percent in RCSs (e.g. ISIS, FNAL and AGS Boosters).

As opposed to the accumulator, the RCSs operating at 30 Hz require a high RF voltage (about 400 kV per ring at 1.4 - 1.9 MHz) for fast acceleration, a large magnet aperture to accommodate the space charge at a lower energy, ceramic vacuum pipes with detailed RF shielding, and high-performance power supplies. Minimization of magnetic errors due to eddy current, ramping, saturation, and power-supply tracking is non-trivial. The study concluded that the required RCS design is technically more demanding and less cost effective [4].

Permanent magnets were considered as an option for the accumulator ring magnets. Electromagnetic magnets were chosen instead, given the uncertainty in the linac energy. This choice is especially appropriate to accommodate later-adopted SRF linac.

Ring's FODO-doublet Lattice

The four-fold symmetric ring lattice contains four dispersion-free straights, each housing injection, collimation, RF, and extraction, as shown in Fig. 4. Each achromatic arc consists of 4 FODO cells with 90° horizontal phase advance.

After optimization, the ring lattice has doublet straights [3]. The lattice combines the FODO structure's simplicity and ease of correction with the doublet structure's flexibility for injection and collimation. In-
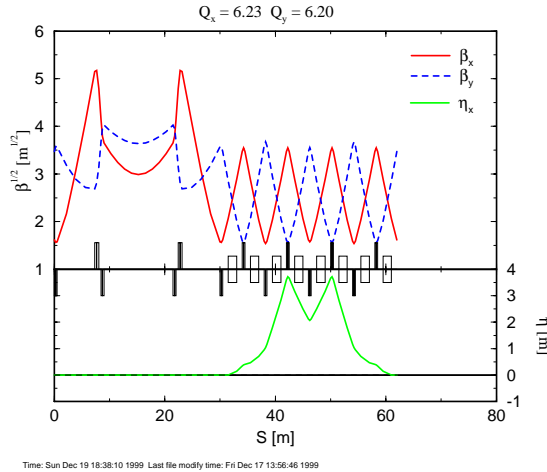
FIGURE 5. SNS ring lattice super-period of FODO/doublet structure. The lattice periodicity is 4.

jection at a dispersion-free region allows independently adjustable painting in the transverse (with orbit bumps in the ring) and longitudinal (with an energy-spreading phase-modulated RF cavity in the HEBT) directions for a robust operation. The 12.5 m-long uninterrupted straight section with a flexible phase advance further improves collimation efficiency. Comparing with the original all-FODO lattice, matching between the arcs and the straights increases the arc acceptance by 50% with the same magnet aperture (Fig. 5).

CHALLENGES & LESSONS LEARNED

Front End & Warm Linac

Tight optical focusing used for chopping and antichopping in a long MEBT is a source of beam-halo generation. Studies show that even without the antichopper, partially deflected particles are still mostly contained by the envelope of the nominal unchopped beam [6]. The MEBT quadrupoles are thus made independently adjustable so that alternative optics can be realized, avoiding tight focusing at the antichopper or MEBT chopper.

Permanent-magnet quadrupoles are used in the DTL due to the tight geometry (402.5 MHz starting at 2.5 MeV), although electromagnetic quadrupoles could be used at DTL tank 3 and beyond. During 1999, the aperture of CCL was reduced from 4 to 3 cm for cost savings. Later when SRF linac is adopted, simulated beam loss often occurs near the end of CCL as the focusing strength is reduced to match the SRF optics.

A key challenge in linac performance is to minimize beam emittance growth and centroid jitter in both transverse and longitudinal directions upon ring injection, reducing foil traversal, scattering and radio-activation. The warm DTL operating at 402.5 MHz is expected to be less
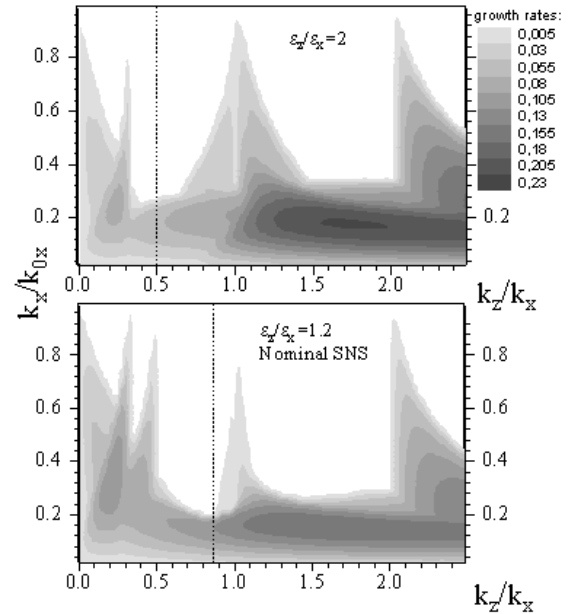
FIGURE 6. Analytical resonance chart showing Instability growth rate due to space-charge coupling resonance. The effects become important only when the transverse and longitudinal tunes are on resonance, and when the emittances differ significantly. The dash lines indicate equipartition.

sensitive to vibrational noises than most existing linacs operating at 200 MHz. A tight RF control ($<0.5\%$ amplitude and $0.5°$ phase error) warrants tolerable energy variation before the beam enters energy correction and spreading cavities in the HEBT [7].

Superconducting RF Linac

Using only two types of cavity β for over 800 MeV of acceleration compromises the equipartition law. Space-charge coupling can cause transverse and longitudinal emittance exchange when the emittance ratio meets resonance conditions (Fig. 6) [8]. In addition, depending on the level of initial mismatch, space-charge parametric halo may develop in the linac. Efforts were made to reserve an economically affordable large aperture, and to reserve tunability in the MEBT, CCL and SRF linac.

Effects of higher-order modes (HOM) on the cavities is another issue. Overlapping of beam and HOM spectrum is possible because of the pulsed time structure of the beam and the fact that the beam frequency shifts with variable ring energy and repetition rate (e.g. for some two-target operation scenarios). Fortunately, transverse and longitudinal (beam break-up) instabilities are minor issues for an ion beam in the presence of a cavity-to-cavity frequency spread [9]. HOM dampers are implemented only for the purpose of power dissipation [10].
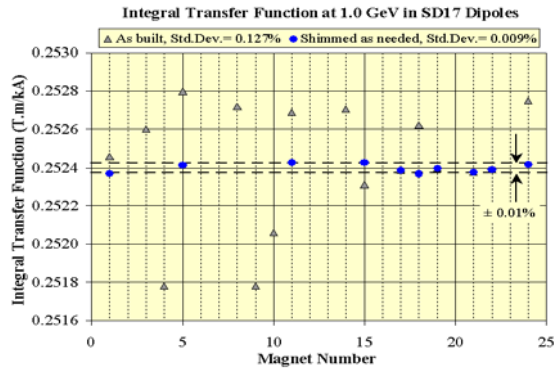
Source: P. Wanderer, A. Jain, et al

FIGURE 7. Variation of integral transfer function of SNS ring dipole magnets before and after shimming. The measurement current corresponds to 1 GeV beam energy.

The SRF linac performance is limited by the available klystrons power (550 kW). Up to 40% RF-power is reserved for compensation of cavity errors (Lorntz detuning, microphonics, coupling loss, frequency setting), klystron loss, and missing-cavity tuning. To reduce such overhead, each SRF cavity is equipped with a piezo crystal driven fast tuner to compensate for the Lorentz force.

Ring and Transport

Solid-steel, as opposed to laminated-steel, was selected for most ring and transport magnet cores for cost savings. Individually, good field quality ($<10^{-4}$ relative error at full acceptance) is achieved. However, excessive (up to 0.25%) magnet-to-magnet variation is found in the dipole transfer function and its current dependence, as shown in Fig. 7 [11]. These dipoles are shimmed to achieve below 10^{-4} variation for 1 GeV operation, and sorted according to 1.3 GeV measurement data to minimize orbit corrector strength.

Main ring challenges include meeting the target requirements on the peak current density, minimizing uncontrolled beam loss, and controlling collective effects (space charge, instabilities, electron cloud (Fig. 8)) [4]. Efforts are made to minimize leading sources of beam-coupling impedance (Fig. 9 [12]), and to enhance Landau damping [4].

High-performance beam diagnostics is needed to accommodate the large variation of beam parameters, and for machine protection across the entire facility. Laser-wire monitors are under test for possible implementation in the SRF linac for a clean operation, and luminescence profile monitors are under test to reduce space-charge and electron-cloud complications in the ring.
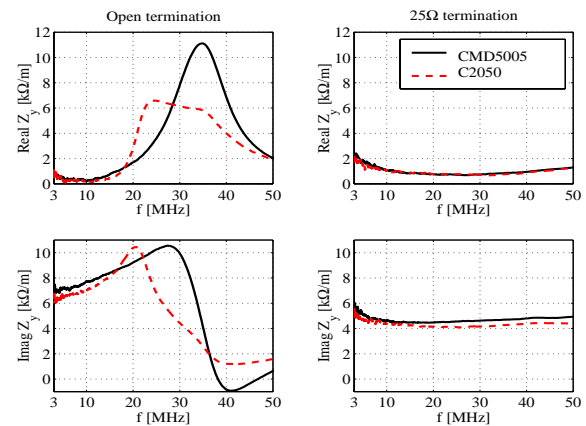
SUMMARY

By adopting superconducting RF technology for the linac and by fully optimizing the accumulator ring de-
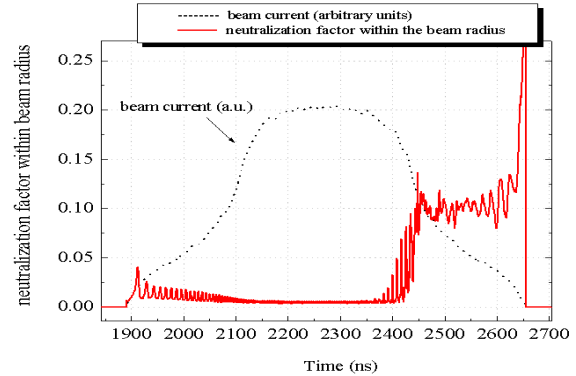
Source: M. Pivi, M. Furman

FIGURE 8. Simulation of single-bunch electron multipacting with a peak secondary-emission yield of 2.

Source: D. Davino, H. Hahn

FIGURE 9. Comparison of bench-measured coupling impedance for open and 25 Ω PFN termination, and high (1600) and medium (100) permeability ferrite of the ring extraction-kicker assembly.

sign, the Spallation Neutron Source project, half way towards its completion, is meeting the challenge to be a next-generation, high-power accelerator facility.

I am indebted to my colleagues, especially those participating in SNS accelerator-physics discussions.

REFERENCES

1. N. Holtkamp, EPAC (2002)
2. N. Catalan-Lasheras et al, SNS Notes SNS/AP/7 (2001)
3. J. Wei et al, Phys. Rev. ST-AB **3**, 080101 (2000)
4. J. Wei et al, EPAC'00, 981; PAC (2001) 319; EPAC (2002)
5. J. Stovall et al, LINAC 2000, p.605
6. D. Jeon et al, SNS 104050000-TD0010-R01 (2002)
7. D. Raparia et al, Workshop HB2002, FNAL (2002)
8. I. Hofmann, et al, PAC (2001) 2902
9. R. Sundelin et al PAC'01 1984; D. Jeon et al, PAC'01 2063
10. S. Kim, et al, PAC (2001) 1128
11. P. Wanderer et al, EPAC (2002)
12. D. Davino et al, EPAC (2002)